Supplemental Data

Single-cell profiling of glomerular cells provides a dynamic picture in experimental diabetic kidney disease

Jia Fu, Kemal M. Akat, Zeguo Sun, Weijia Zhang, Detlef Schlondorff, Zhihong Liu, Thomas Tuschl, Kyung Lee, and John Cijiang He

Supplemental Figures 1-15

Supplemental Table 1-2

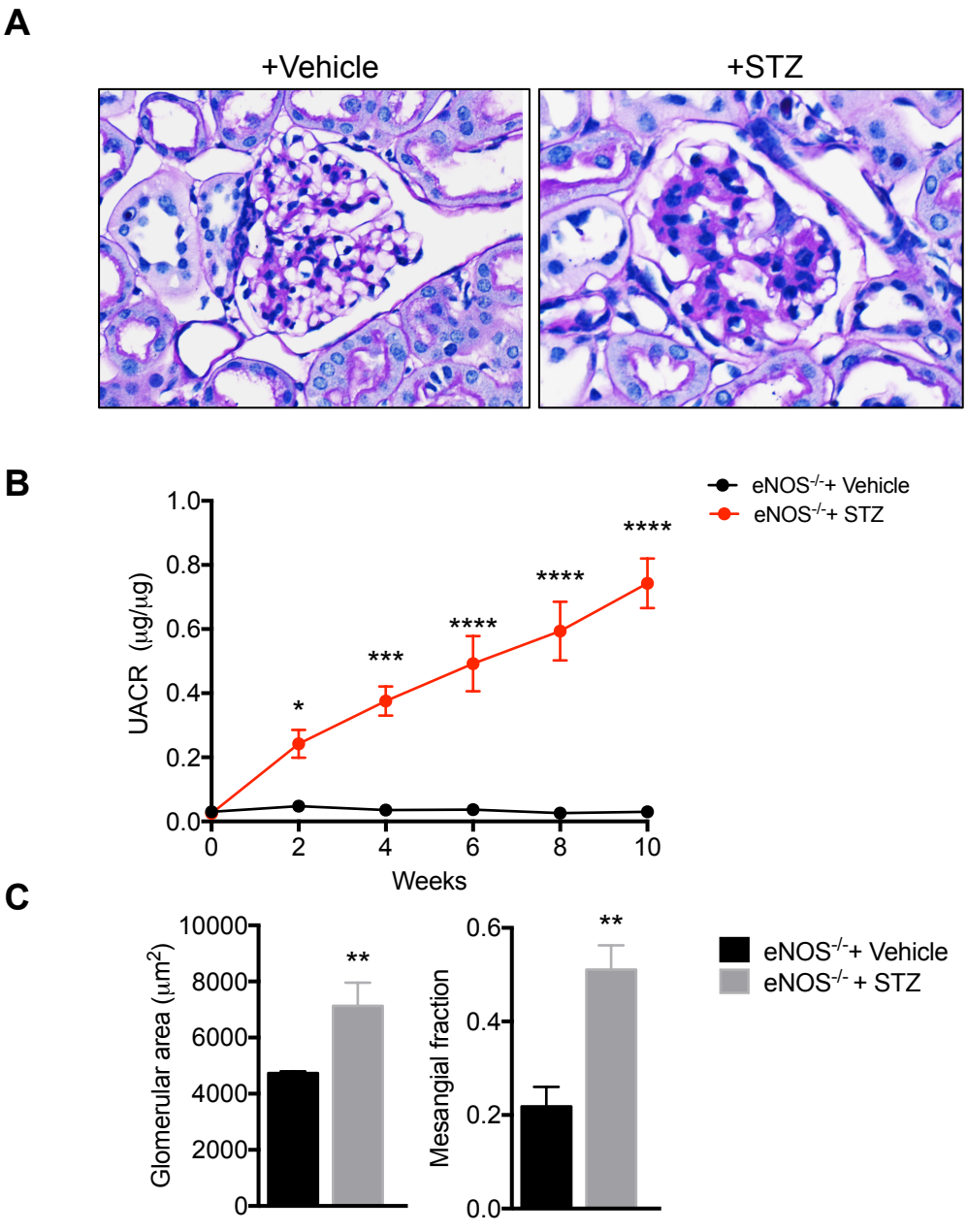

Supp. Fig. 1: Characterization of eNOS$^{-/-}$ mice at 10 weeks of diabetes induction. (A) Representative images of periodic-acid Schiff-stained kidney sections of eNOS$^{-/-}$ mice injected with either citrate buffer (+Vehicle) or with streptozotocin (+STZ) at 10 weeks post-injection. 200x magnification. (B) Urinary albumin to creatinine ratio (UCAR) shows the development of proteinuria in the diabetic of eNOS$^{-/-}$ mice. (C) Glomerular area and mesangial fraction are increased in the diabetic eNOS$^{-/-}$ mice. n=3, *P<0.05, **P<0.01, ***P<0.001, and ****P<0.0001 when compared with vehicle-treated controls.

Exp #1

	Column 1	Column 2	Column 3	Column 4	Column 5	Column 6	Column 7	Column 8	Column 9	Column 10	Column 11	Column 12	Column 13	Column 14	Column 15	Column 16	Column 17	Column 18	Column 19	Column 20
Row 1	1	0	1	1	1	1	0	1	0	1	1	1	1	1	1	1	0	1	2	1
Row 2	1	0	1	0	2	1	0	1	1	1	1	1	1	0	1	0	1	2	1	0
Row 3	1	1	0	1	1	1	1	0	1	1	1	1	0	0	1	1	1	0	1	1
Row 4	1	0	1	2	2	0	0	1	1	1	1	1	1	1	1	1	1	0	1	1
Row 5	1	1	0	1	1	1	0	0	1	1	0	1	1	0	1	1	1	0	1	1
Row 6	1	1	1	1	1	1	1	1	1	1	2	0	1	1	1	1	2	1	1	0
Row 7	2	0	1	1	1	1	0	1	0	1	1	1	1	1	1	1	1	1	1	0
Row 8	2	1	1	1	1	1	1	1	0	1	1	1	1	1	1	0	1	1	1	0
Row 9	1	1	0	1	1	1	1	1	1	1	1	0	1	1	1	1	1	0	1	0
Row 10	1	1	1	1	1	1	1	0	1	0	1	1	1	1	0	0	1	1	0	0
Row 11	1	1	1	1	1	1	1	1	1	1	1	1	1	1	1	0	1	1	1	1
Row 12	1	0	1	1	1	1	2	1	0	1	0	1	1	1	0	1	1	1	1	1
Row 13	1	1	1	1	1	1	0	1	0	2	1	1	0	1	1	0	1	1	1	1
Row 14	1	1	0	1	1	1	1	0	1	1	0	1	1	1	1	0	2	1	1	1
Row 15	1	1	1	1	0	1	1	1	1	1	0	1	1	1	1	1	1	1	0	0
Row 16	1	1	1	0	1	1	0	1	1	1	1	1	1	1	1	1	1	0	1	1
Row 17	1	1	1	1	1	1	1	1	1	1	0	1	1	1	1	1	1	1	0	1
Row 18	1	1	1	1	1	1	1	1	0	0	1	1	1	1	0	1	1	1	0	0
Row 19	1	0	1	1	1	1	1	1	1	0	1	0	1	1	1	2	1	1	1	0
Row 20	1	1	1	3	1	1	1	1	1	0	1	0	1	0	1	1	1	0	1	1
Row 21	1	0	1	1	1	0	1	1	1	1	0	1	1	1	1	1	1	1	1	1
Row 22	1	0	1	1	1	1	0	1	0	1	0	1	1	0	0	0	1	1	1	0
Row 23	0	0	1	1	1	1	1	1	1	1	1	1	1	1	1	1	2	1	1	1
Row 24	0	1	1	1	1	1	1	1	1	2	1	1	1	1	1	1	1	1	1	0
Row 25	1	1	1	1	1	1	1	1	1	1	1	1	1	1	1	1	0	1	1	1
Row 26	1	1	1	1	2	1	1	1	0	0	1	1	1	1	1	1	1	0	1	1
Row 27	1	1	1	0	1	1	1	1	1	1	1	1	1	1	1	0	1	0	1	0
Row 28	1	1	1	1	1	1	1	1	1	1	1	1	0	1	1	1	1	1	1	0
Row 29	1	1	1	2	1	1	1	1	1	1	1	1	1	1	0	1	1	2	1	0
Row 30	1	1	1	1	1	1	0	1	0	1	1	1	1	1	2	1	2	1	1	1
Row 31	0	0	1	1	1	1	1	1	1	1	1	1	1	0	2	1	1	0	1	0
Row 32	0	0	1	1	1	0	1	1	1	0	1	1	1	1	2	0	1	1	1	1
Row 33	1	1	1	1	0	1	0	1	1	0	0	0	1	1	2	1	1	1	1	1
Row 34	1	0	1	1	1	1	1	1	1	1	0	1	1	1	0	1	1	1	1	1
Row 35	1	1	1	1	1	1	1	1	1	1	0	1	1	1	2	0	1	1	1	1
Row 36	1	1	1	1	1	1	0	1	0	0	1	1	1	2	0	1	0	1	0	0
Row 37	1	0	1	0	1	1	1	1	0	0	0	1	1	0	2	1	1	1	0	0
Row 38	1	0	1	1	1	1	1	1	1	1	0	1	1	1	0	0	0	1	1	1
Row 39	1	1	1	1	2	0	0	1	1	0	1	1	1	0	1	1	0	1	0	1
Row 40	1	1	1	0	1	1	1	1	1	1	1	1	0	0	1	0	1	1	1	1
Single-cell:	34	26	36	32	34	36	27	36	29	28	27	35	36	30	26	27	31	29	32	23
				Diabetic				Columns 1-10		318					Control			Columns 11-20		296

Exp #2

	Column 1	Column 2	Column 3	Column 4	Column 5	Column 6	Column 7	Column 8	Column 9	Column 10	Column 11	Column 12	Column 13	Column 14	Column 15	Column 16	Column 17	Column 18	Column 19	Column 20
Row 1	0	1	0	1	1	1	0	1	2	1	1	2	0	1	1	0	1	1	1	1
Row 2	1	1	3	0	0	1	1	0	1	0	1	1	0	1	2	1	1	0	0	0
Row 3	1	1d	1	0	1	de	1	de	3	0	1	de	1	1	1	0	3	0	1	0
Row 4	0	1	1	2	1	2	1	0	1	0	1	0	1	1	1	0	2	0	0	0
Row 5	0	1	1	0	0	1	0	de	1	1	1	2	1	1	1	0	1	1	0	0
Row 6	3	1	2	1	1	1	1	0	1	1	1	0	0	5	1	0	1	2	1	2
Row 7	0	1	1	1	de	1	1	1	1	1	1	0	1	1	1	2	1	0	0	1
Row 8	0	1	1	0	1	0	0	de	1	0	1	0	0	1	0	0	0	2	1	2
Row 9	0	0	0	3	0	1	0	de	1	0	1	1	0	1	1	0	0	1	1	0
Row 10	1	3	1	1	1	0	1	1	1	1	0	1	1	0	1	1	1	0	0	0
Row 11	de	1	1	1	1	2	1	1	1	1	1	1	0	0	1	1	de	1	de	1
Row 12	0	1	1	1	1	0	1	1	1	de	1	0	0	0	0	1	1	1	1	1
Row 13	0	1	1	1	0	1	0	1	1	1	2	0	1	1	1	2	0	0	2	1
Row 14	1	2	0	1	1	0	1	1	1	1	1	1	1	1	0	0	0	1	1	1
Row 15	0	1	1	0	1	1	0	0	1	1	1	1	1	0	0	1	2	3	1	1
Row 16	0	1	3	1	de	0	1	de	1	1	1	1	1	0	0	1	1	0	3	1
Row 17	1	1	1	1	1	0	1	de	0	0	1	0	0	0	2	0	2	1	0	1
Row 18	3	1	1	1	1	1	de	1	0	1	2	0	1	0	2	0	2	0	2	1
Row 19	0	0	1	1	0	1	0	0	1	1	de	de	1	2	1	1	1	0	2	1
Row 20	1	1	1	0	1	1	0	1	0	1	1	1	de	0	1	0	0	0	1	0
Row 21	0	1	1	1	1	1	2	1	1	1	1	0	1	0	1	1	1	1	3	1
Row 22	2	5	1	1	1	1	2	1	1	1	1	1	1	1	0	1	1	1	1	1
Row 23	0	0	1	1	1	0	2	1	0	0	0	0	1	1	de	1	2	de	2	0
Row 24	1	5	3	0	0	de	1	de	de	1	1	de	1	0	1	1	1	1	0	0
Row 25	1	0	0	1	1	1	1	1	2	1	1	1	de	1	1	0	1	0	1	0
Row 26	0	1	1	0	1	1	1	1	2	1	1	0	1	0	1	3	1	1	1	1
Row 27	1	1	0	1	2	de	1	1	1	de	1	1	1	3	1	0	2	1	1	2
Row 28	0	1	1	1	1	1	0	1	1	de	0	1	0	1	1	1	1	0	1	0
Row 29	1	1	1	5	1	de	0	1	1	1	2	1	1	3	de	2	2	1	1	1
Row 30	2	3	1	1	1	de	0	1	0	1	1	0	1	1	1	1	0	de	1	1
Row 31	1	1	0	1	0	1	1	1	1	1	1	1	1	1	2	0	2+de	0	1	1
Row 32	0	3	1	1	1	1	0	1	2	1	1	1	1	1	de	1	1	1	1	5
Row 33	1	1	0	1	2	1	1	1	1	0	2	1	1	0	3	0	1	0	0	0
Row 34	0	1	1	1	0	2	de	0	1	0	1	1	0	1	1	1	0	0	1	2
Row 35	0	0	0	1	1	0	1	2	de	1	1	1	2	0	1	0	2	shadow	0	0
Row 36	0	1	0	1	1	de	1	0	1	1	1	0	2	1	1	2	0	1	1	5
Row 37	1	1	0	de	1	0	0	1	2	1	1	2	1	3	1	1	1	1	1	1
Row 38	2	1	1	1	2	1	1	1	1	1	2	3	2	0	3	0	1	5	1	3
Row 39	2	2	0	1	0	1	1	1	1	1	2	1	1	1	3	1	1	0	1	1
Row 40	0	2	0	de	0	de	1	1	1	1	1	0	1	0	1	1	1	de	1	1
Single-cells	13	26	24	27	25	21	22	25	27	28	30	19	25	20	24	18	21	16	24	20
				Diabetic				Columns 1-10		238					Control			Columns 11-20		217

Supp. Fig. 2: Assignment of captured cells on IFC. All cells captured for experiment 1 (top) and experiment 2 (bottom) were visualized using a microscope compatible with IFC. “1” refers to a single cell observed in the capture site; “0” to no cell seen; “de” to cell debris; and any number greater than 1 to multiple cells visualized.

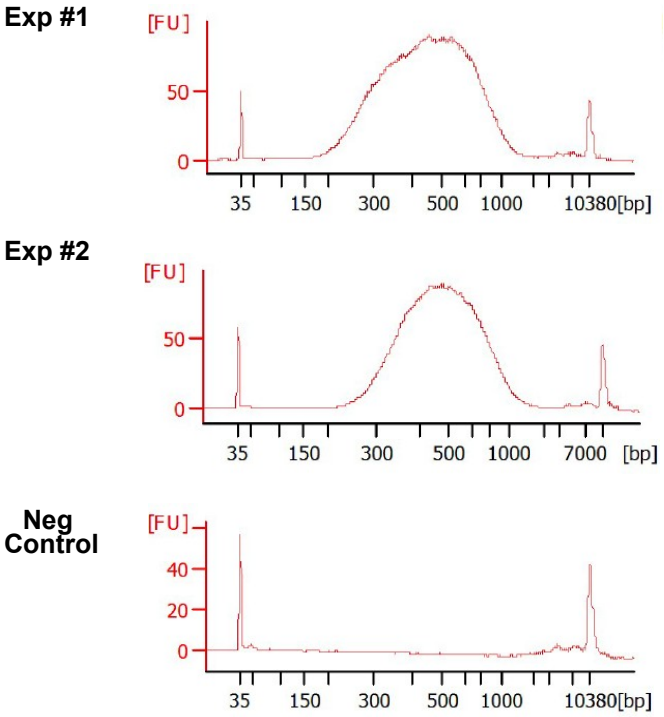

Supp. Fig. 3: Analysis of single-cell cDNA library preparation on the Fluidigm C1 platform. The Agilent Bioanalyzer analysis of glomerular cell cDNA library sample from the two experiments and the negative control (no input) are shown.

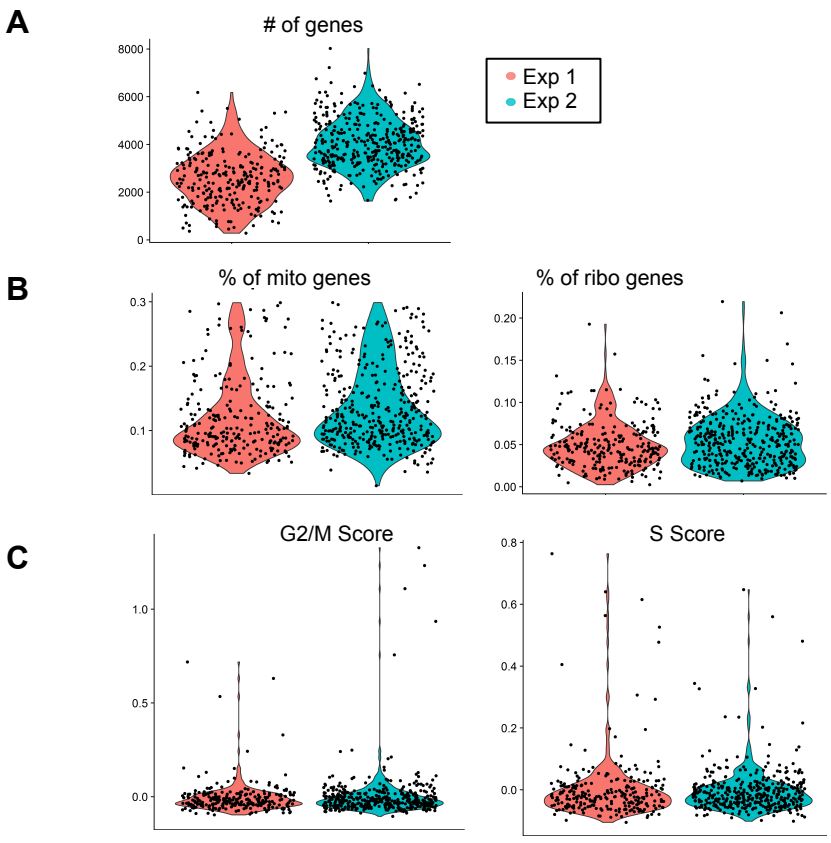

Supp. Fig. 4: Quality control plots for the two scRNA-seq experiments. Violin plots showing number of genes (A), percentage of mitochondrial (mito) and ribosomal (ribo) genes (B), and G2M and S score (C) for cells in two independent experiments (Exp1 an Exp2). External RNA controls consortium (ERCC) spike-in standard was included in Exp1 and omitted in Exp2, resulting in increased sequencing depth, as shown in (A).

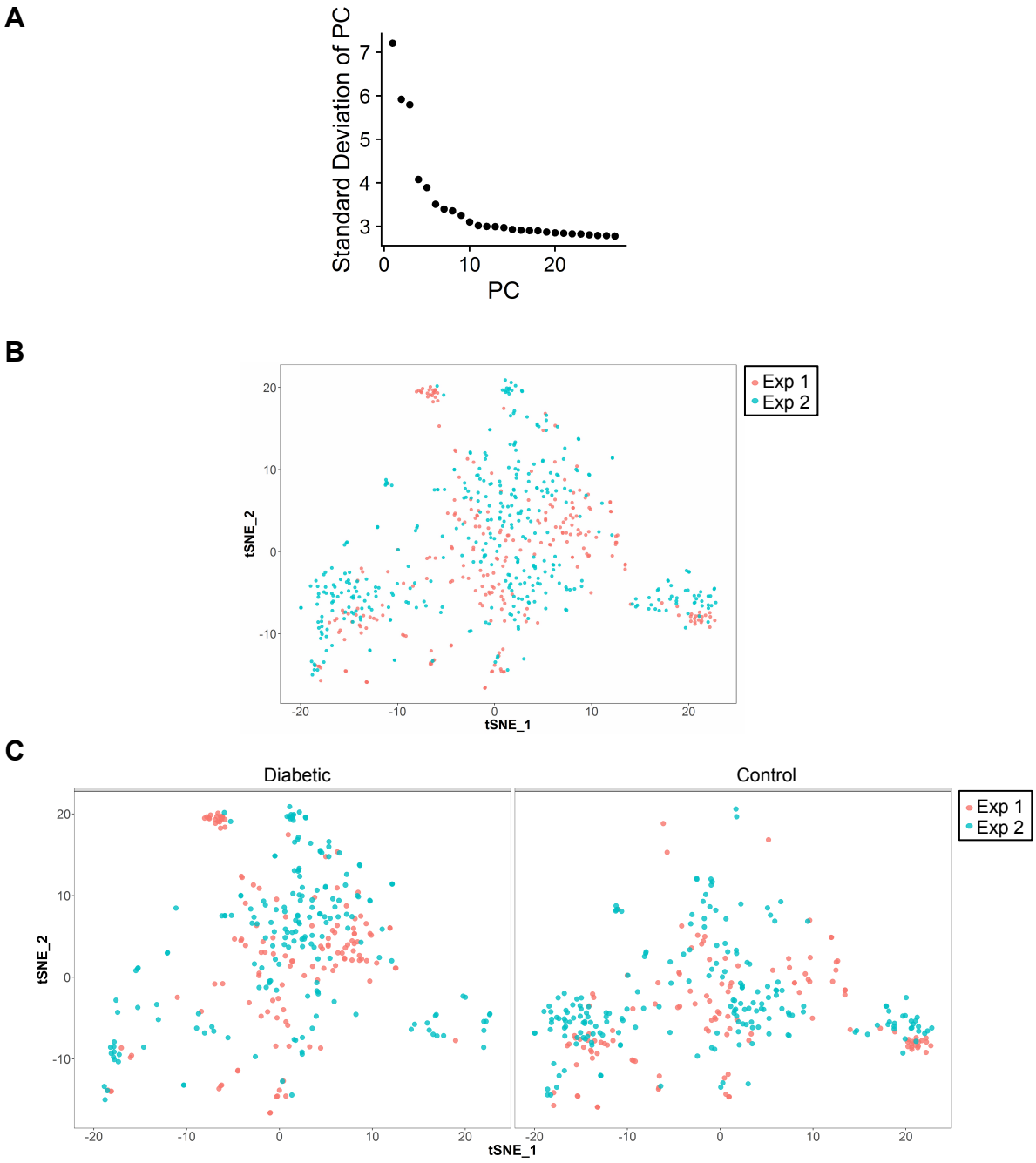

Supp. Fig. 5: Unsupervised clustering of single-cells. (A) Standard deviations of the top 27 principle components are shown. The top 15 principal components were chosen for cell clustering and t-SNE projection, since no significant changes were observed beyond 15 principal components. (B-C) t-SNE analysis of two replicate experiments (red dots, cells from Exp 1; blue dots, cells from Exp 2) demonstrating similar clustering of all glomerular cells (B) or separated by control (right panel) versus diabetic (left panel) groups (C).

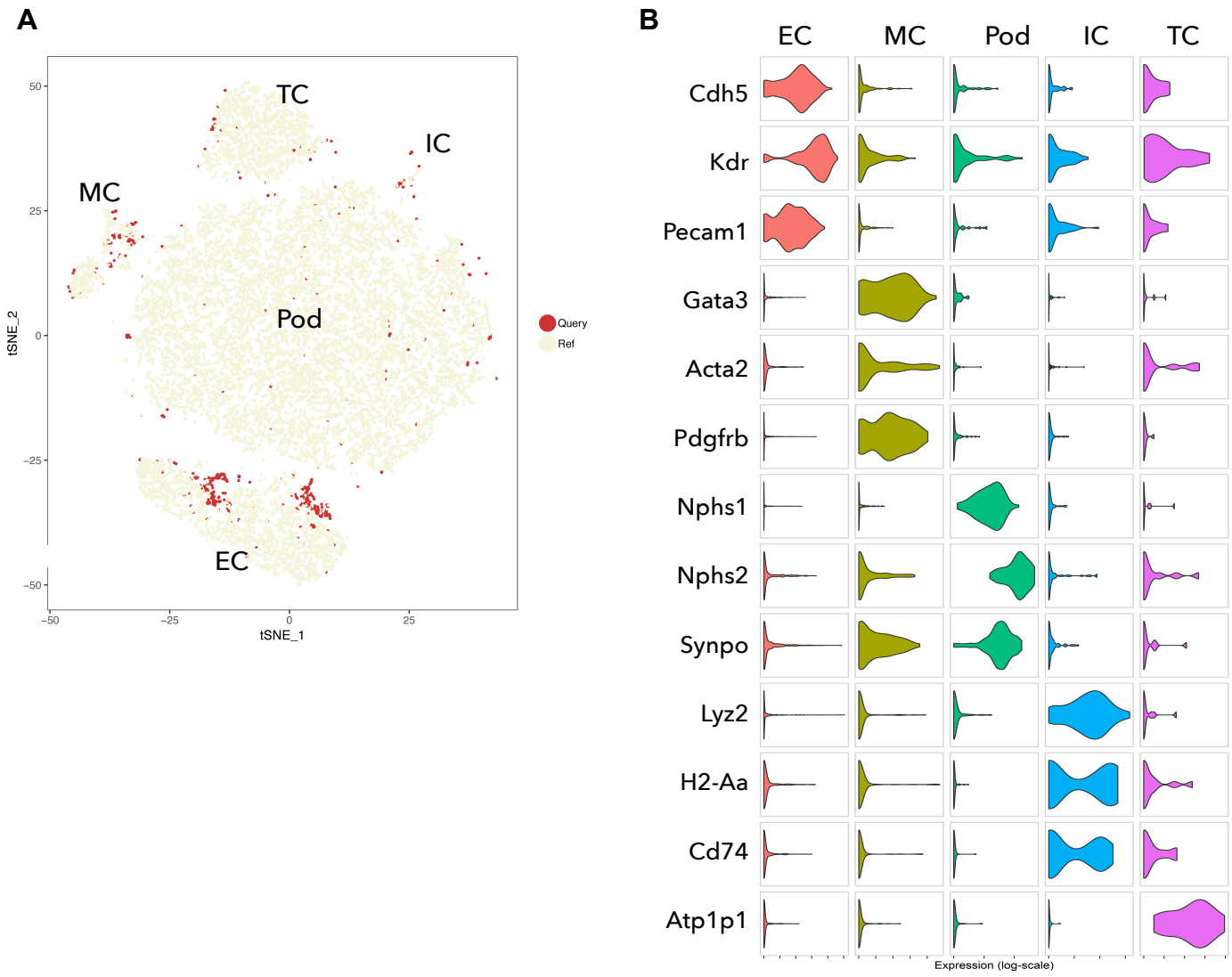

Supp. Fig. 6: **Glomerular single-cell cluster identification.** (A) Consensus clustering of the single-cell sequencing data (red) with reported mouse glomerular single-cell data (beige) from Karaikos *et al.* (B) Violin plots showing expression of established markers for endothelial cells (EC), mesangial cells (MC), podocytes (Pod), tubular cells (TC) and immune cells (IC).

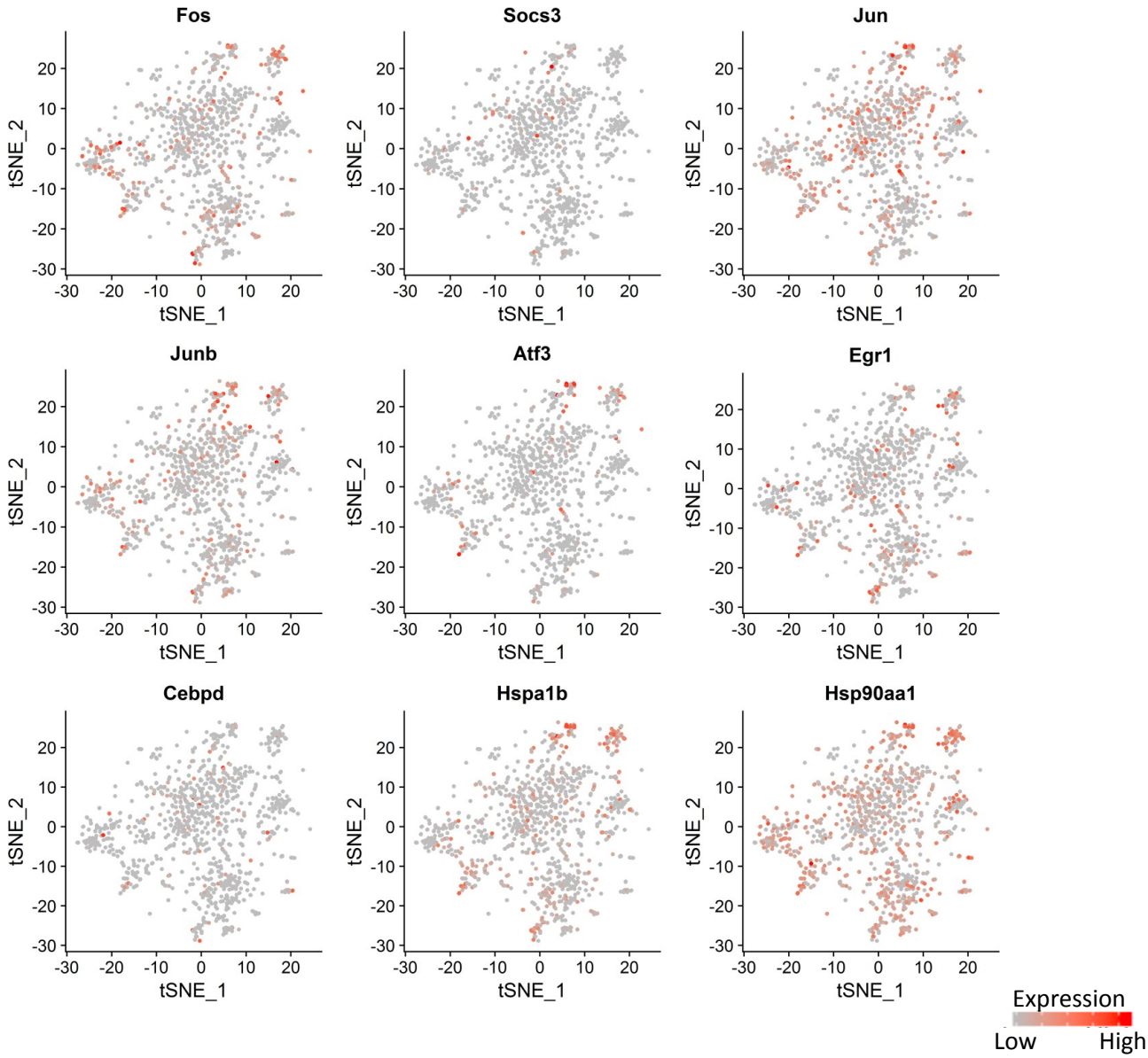

Supp. Fig. 7: Expression of tissue dissociation stress-related genes. Expression levels of genes that are associated with tissue dissociation from van den Brink *et al.* Color key denotes the normalized average expression value of selected differentially expressed genes.

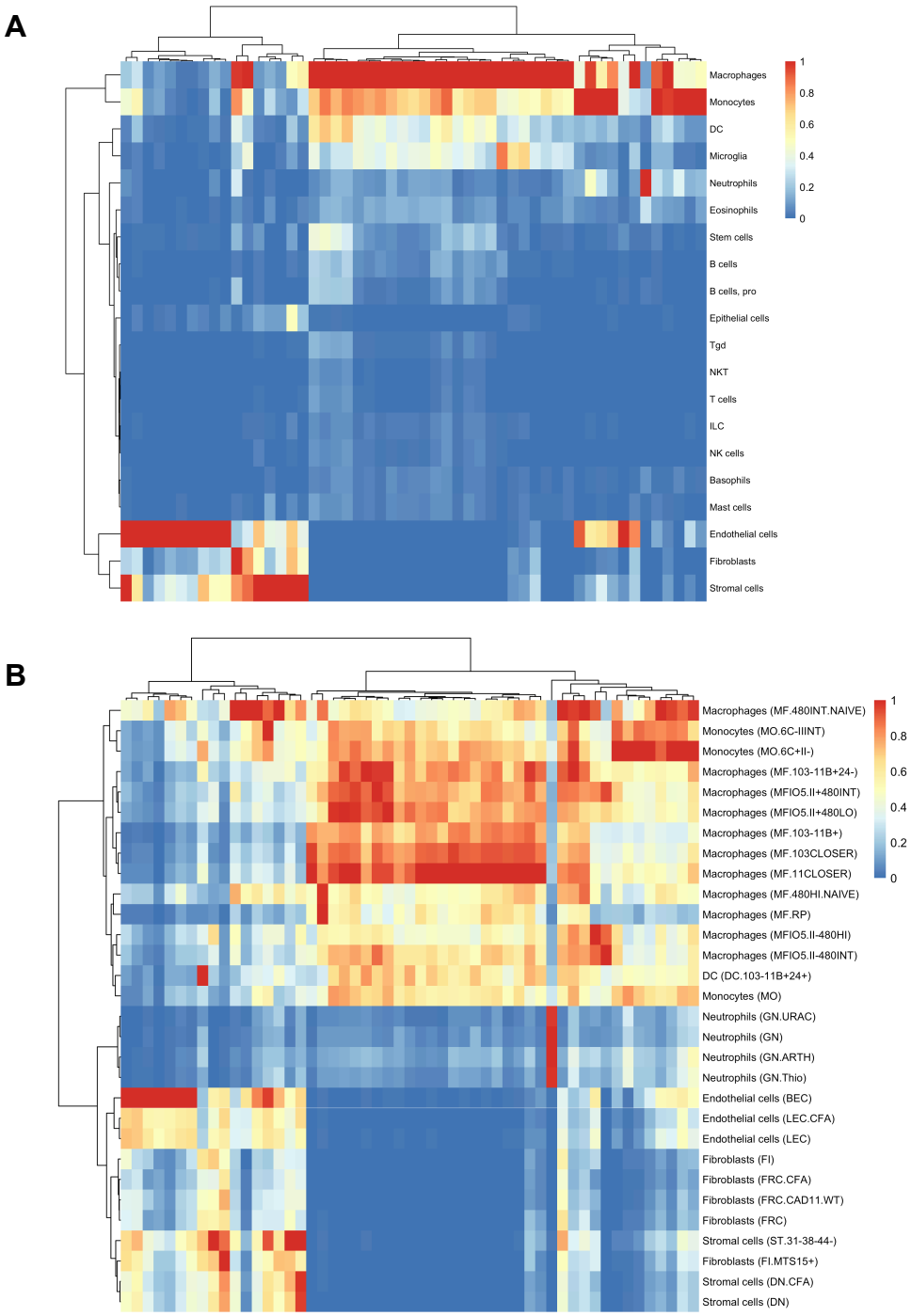

Supp. Fig. 8: Annotation of immune cell cluster. Heatmap of SingleR scores for top correlated (A) main cell types and (B) fine-tuned subtypes as compared to previously published datasets (GSE15907 and GSE37448). Each row corresponds to a cell type and each column corresponds to one cell. Scores were normalized per cell (column); higher score (red) indicates higher correlation.

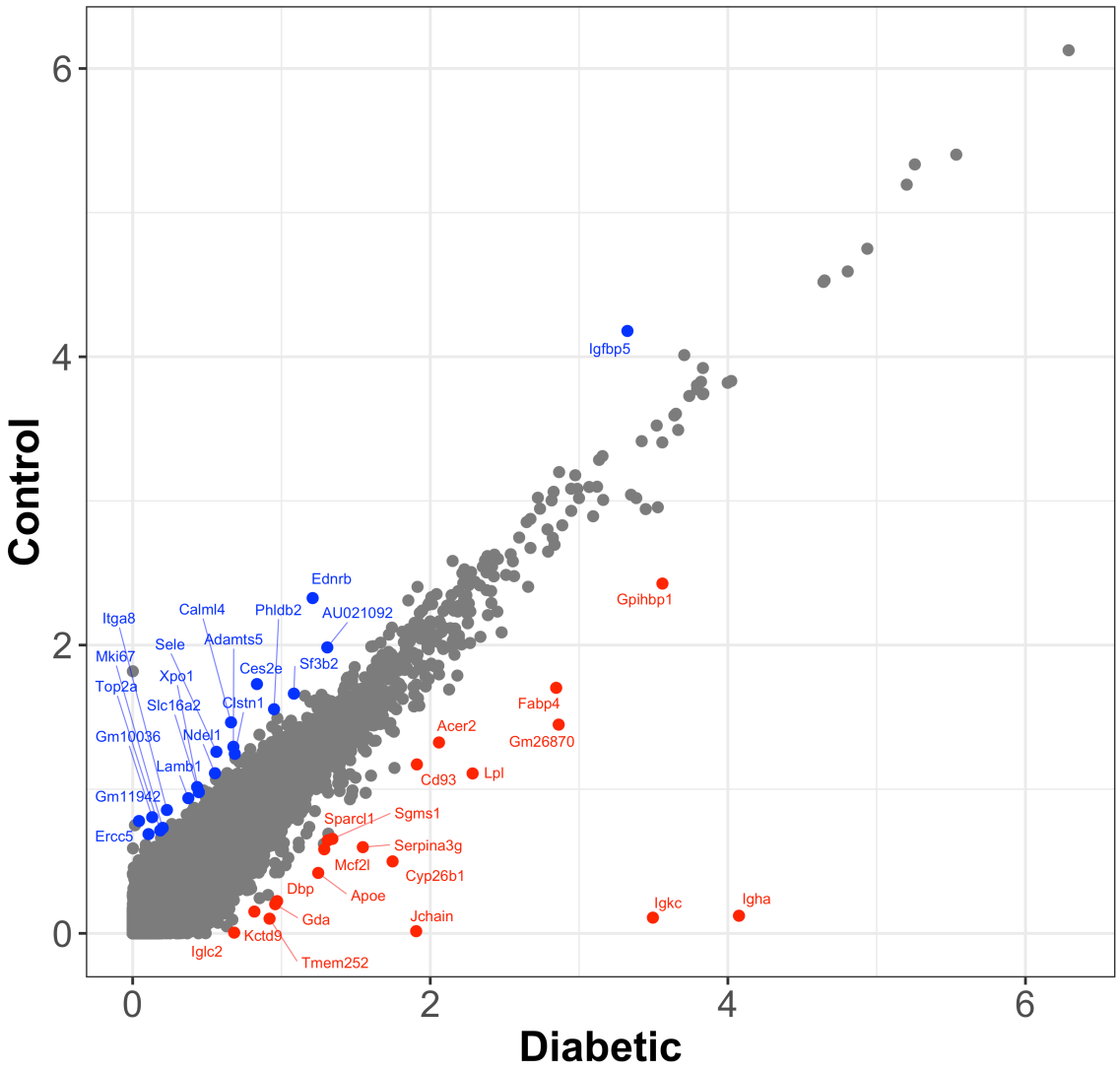

Supp. Figure 9: **DEGs in endothelial cells in glomeruli of diabetic mice.** The top variable genes in log-fold-change with p-value less than 0.05 are highlighted in red for up-regulated genes and in blue for downregulated genes in diabetic mice.

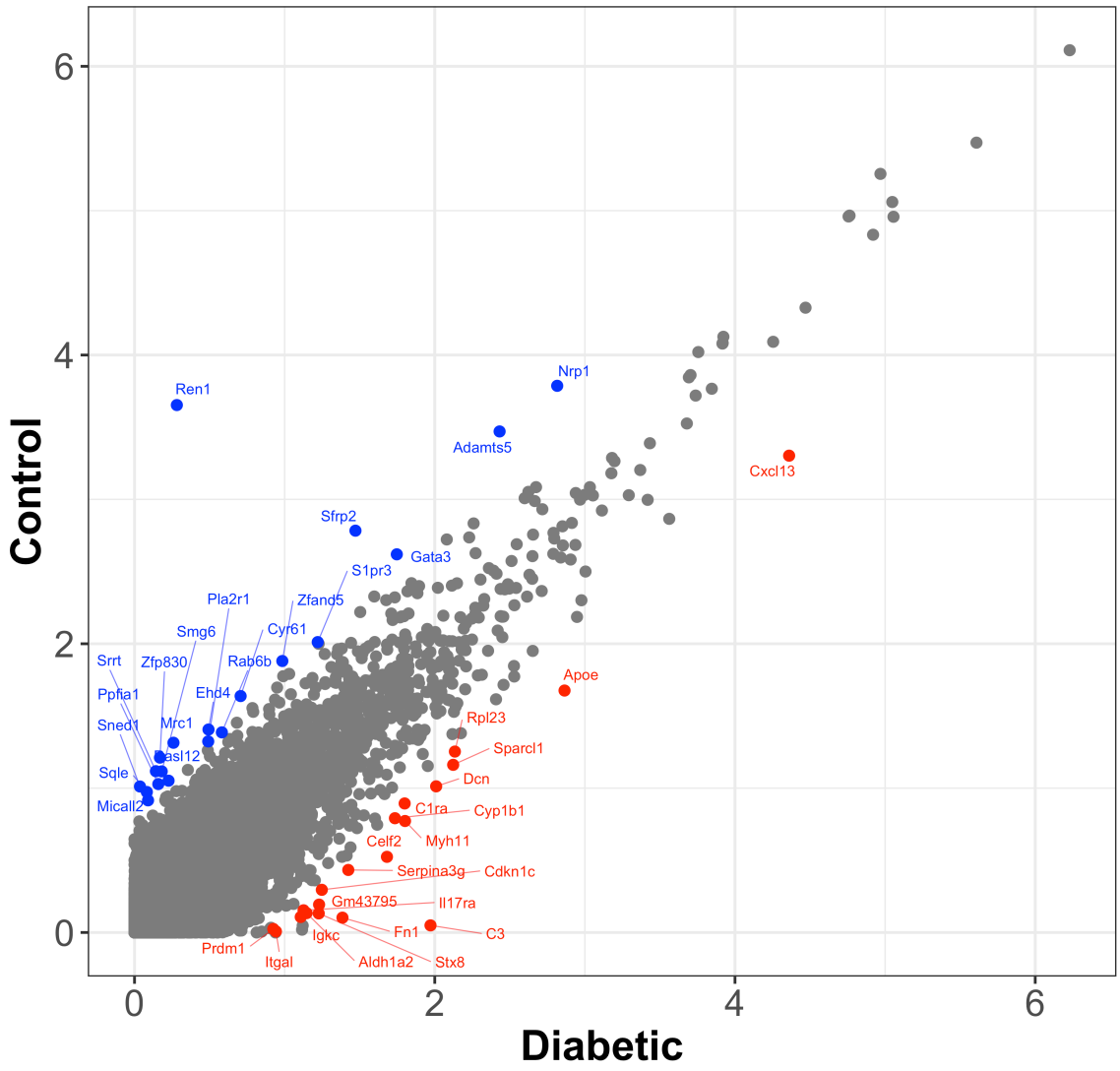

Supp. Figure 10: **DEGs in mesangial cells in glomeruli of diabetic mice.** The top variable genes in log-fold-change with p-value less than 0.05 are highlighted in red for up-regulated genes and in blue for downregulated genes in diabetic mice.

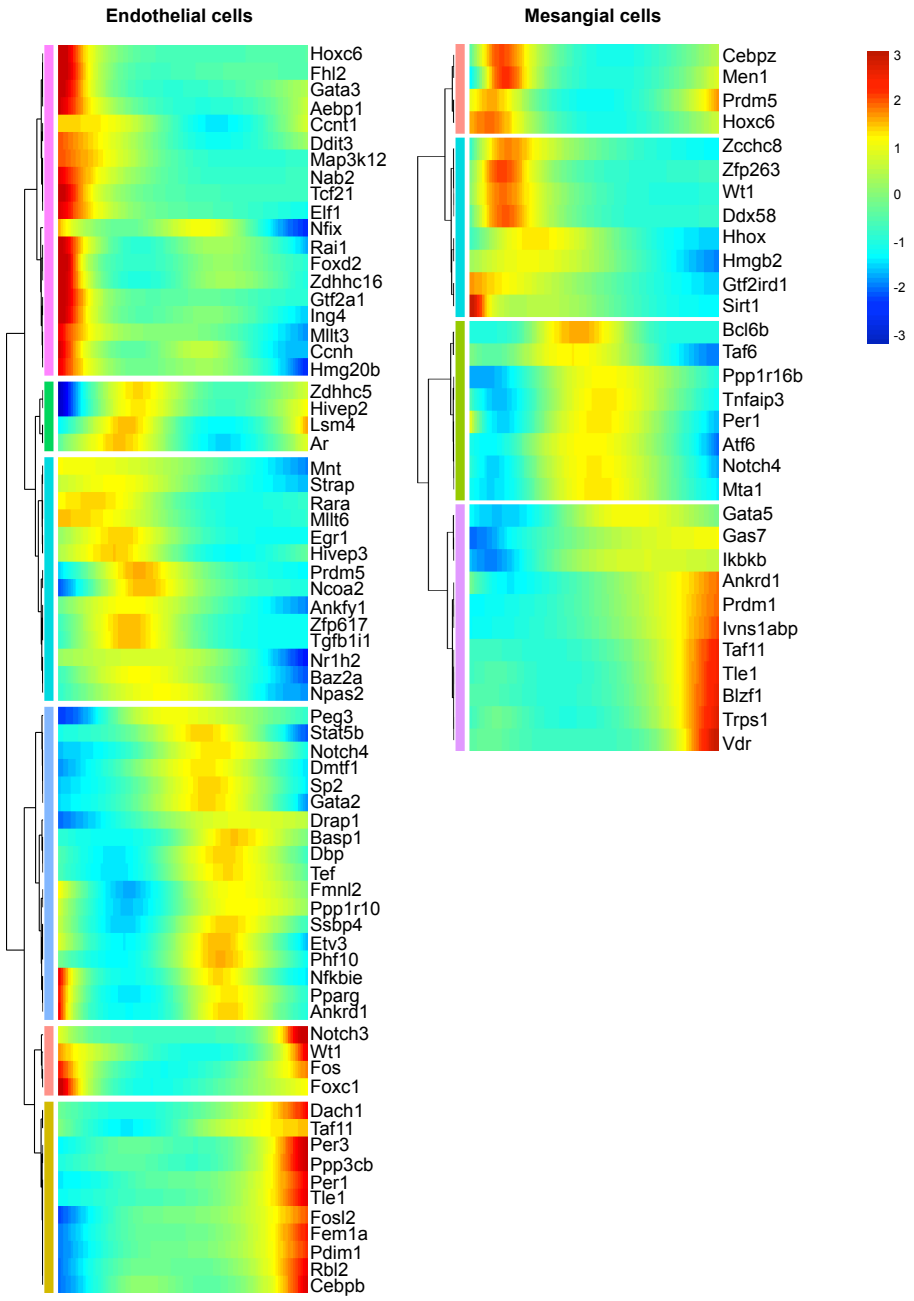

Supp. Fig. 11: Expression of transcription factors in control and diabetic kidney samples in pseudotime. Heatmap plots highlighting examples of transcription factors with expression changes over the course of control-to-diabetes transition for endothelial (Left) and mesangial cell cluster (Right). Each row represents a gene, where the left end corresponds to transition starting point (control); the right end corresponds to transition ending point (diabetes); and the middle indicates transition progress. Color scheme represents the z-score distribution from -3.0 (blue) to 3.0 (red). Genes that co-vary across transition are clustered into blocks. Z score is the number of standard deviations from the mean a data point is.

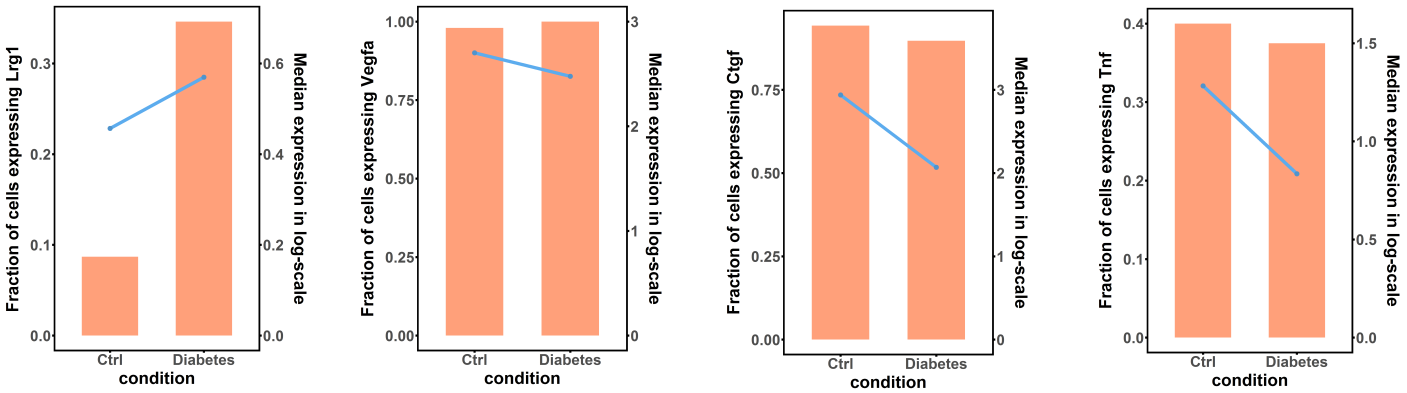

Supp. Fig. 12: Gene expression and expressed cell fraction changes of glomerular cells in diabetic mice. Barplots representing both fraction of cells (orange columns) expressing *Lrg1* in endothelial cells, *Vegfa* in podocytes, *Ctgf* in mesangial cells, and *Tnfa* in immune cells, and median of their expression value (blue dots) in control (Ctrl) and diabetic (Diabetes) mice.

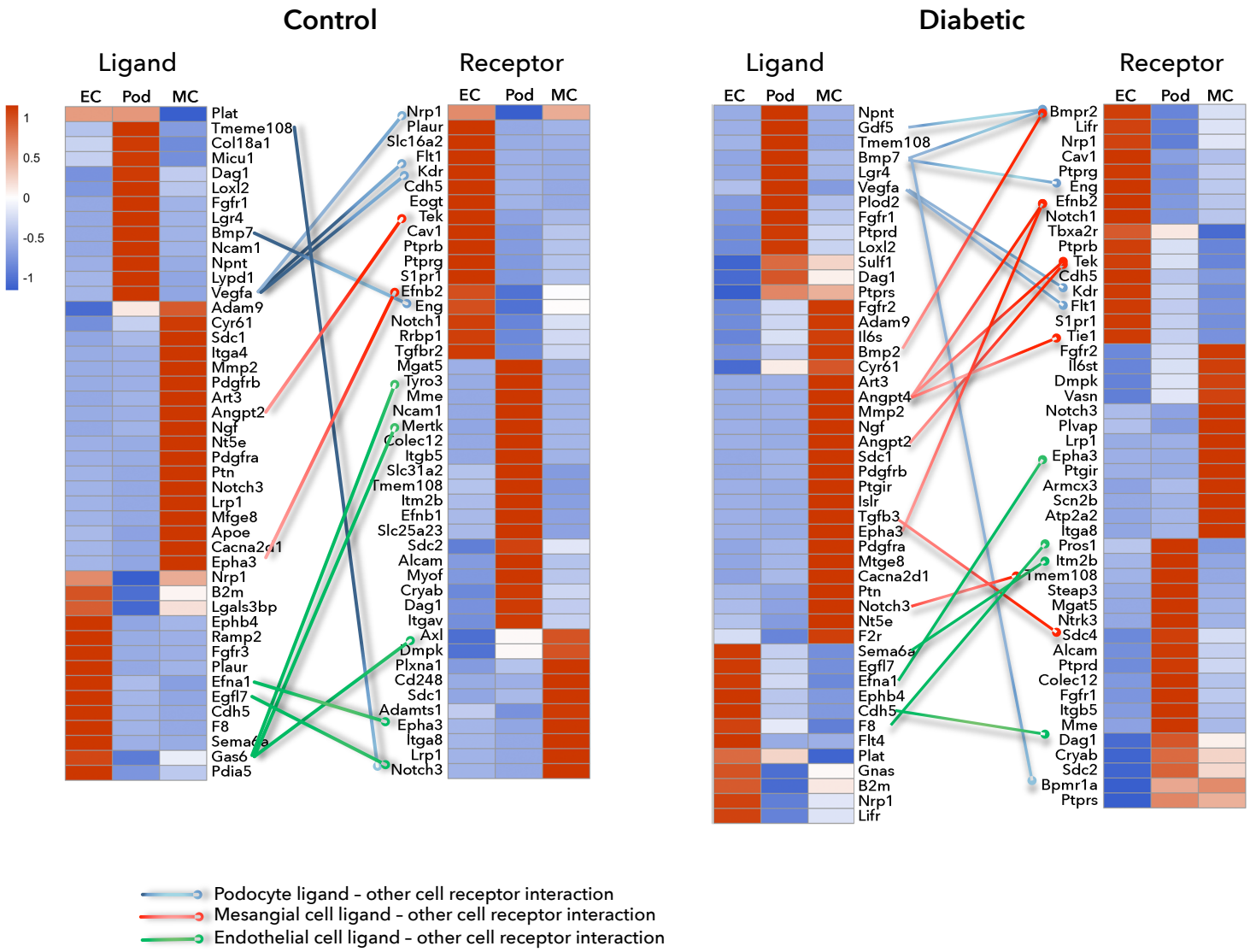

Supp. Fig. 13: Analysis of cellular cross talk via ligand-receptor interactions. Heatmap showing the potential ligand-receptor pair expression (connected by straight lines) according to cell type in control and diabetic mice. Scale shows the calculated z-scores of expression.

Supplemental Tables

Supp. Table 1: Number (n) and % of cells in each cluster from control and diabetic mice

	Control (n)	Diabetic (n)	Control (%)	Diabetic (%)
Endothelial cells	161	208	49.39	65.40
Mesangial cells	105	39	32.21	12.26
Podocyte	50	16	15.34	5.03
Immune cells	5	48	1.53	15.09
Tubular cells	5	7	1.53	2.20
Total	326	318		

Supp. Table 2: Number (n) and % of cells from the two experiments

	Control (n)		Diabetic (n)		Control (%)		Diabetic (%)	
	Exp1	Exp2	Exp1	Exp2	Exp1	Exp2	Exp1	Exp2
Endothelial cells	62	99	90	118	50	49	69.2	62.7
Mesangial cells	34	71	11	28	27.4	35.1	8.5	14.9
Podocyte	22	28	1	15	17.7	13.8	0.76	7.9
Immune cells	3	2	22	26	2.4	1	16.9	13.8
Tubular cells	3	2	6	1	2.4	1	4.6	0.53
Total	124	202	130	188				